

Supplementary Materials: Exploring the Limits of the Geometric Copolymerization Model

1 Martin S. Engler, Kerstin Scheubert, Ulrich S. Schubert and Sebastian Böcker

2 1. Monte-Carlo simulation parameters

Table S1. Initial concentrations (in mol·L⁻¹) and reaction rates of the Monte-Carlo simulations of living polymerizations.

Dataset	Initial concentration			Reaction rates			
	[I] ₀	[A] ₀	[B] ₀	k _{AA}	k _{AB}	k _{BA}	k _{BB}
$DP_n = 3, r_A = 0.01$	1	1	2	0.01	1	0.01	1
$DP_n = 3, r_A = 1$	1	1	1	1	1	1	1
$DP_n = 3, r_A = 2$	1	1	2	2	1	2	1
$DP_n = 25, r_A = 2$	1	10	15	2	1	2	1
$DP_n = 45, r_A = 2$	1	20	25	2	1	2	1

3 2. Independence of the parameter order

4 In the following, let the matrix M of size $n \times m$ be a copolymer fingerprint, in which entry $M_{a,b}$
 5 gives the relative abundance of a copolymer with a monomers of type A and b monomers of type
 6 B. Let T be the number of synthesis steps. Let p_M be the probability of encountering a monomer,
 7 and let p_A be a vector of size T with the probabilities that the encountered monomer is an A for each
 8 synthesis step $1 \leq t \leq T$. Let $p_B(t)$, the probability of encountering a monomer B be defined as
 9 $p_B(t) = 1 - p_A(t)$.

10 Let $\pi(x)$ be a permutation of some vector x . Let M^π be the resulting fingerprint of our model
 11 with input $\pi(p_A)$. We define a model to be *order-independent* if the resulting fingerprints are the same
 12 for any permutation of p_A , that is $M = M^\pi$ for any π .

13 In our previous paper, we introduced a copolymerization model with several variants similar
 14 to a discrete Markov-chain, that append monomers in each synthesis (time) step with Bernoulli or
 15 geometrically distributed probability [1]. Here, we will investigate if they are order-independent.

16 We do a simple experiment to investigate the order-independence of our models. For both
 17 models, we compute a fingerprint with parameters $p_A = [0, 0.1, 0.2, 0.4, 0.5]$, $p_M = 0.5$ and varying
 18 reactivity ratios. Subsequently, for all permutations $\pi(p_A)$ we compute a fingerprint and calculate
 19 the normalized root mean square error (NRMSE) in comparison to the first fingerprint (Fig. S1).

20 The distance between two fingerprints increases with the distance between p_A and $\pi(p_A)$.
 21 However, as the reactivity ratios approach one, the distance between the fingerprints decreases. In
 22 this experimental instance, we see that the models are order-independent if the reactivity ratios are
 23 one.

24 To verify that the models are order-independent for reactivity ratios of one, we investigate the
 25 model variants without reactivity parameters. As previously described by Engler *et al.* [1], for the
 26 Bernoulli model without reactivity parameters, an entry $M_{a,b}$ in the fingerprint M at synthesis step t
 27 for $a > 0$, $b > 0$, and $1 \leq t \leq T$ is given by:

$$\begin{aligned}
 M_{a,b}(t) = & p_M \cdot p_A(t) \cdot M_{a-1,b}(t-1) \\
 & + p_M \cdot p_B(t) \cdot M_{a,b-1}(t-1) \\
 & + (1 - p_M) \cdot M_{a,b}(t-1)
 \end{aligned} \tag{1}$$

28 For the Geometric model without reactivity parameters, we first have to derive a closed form for
 29 $M_{a,b}$. Let $p_G(k)$ be the geometrically distributed probability of adding k monomers in one synthesis

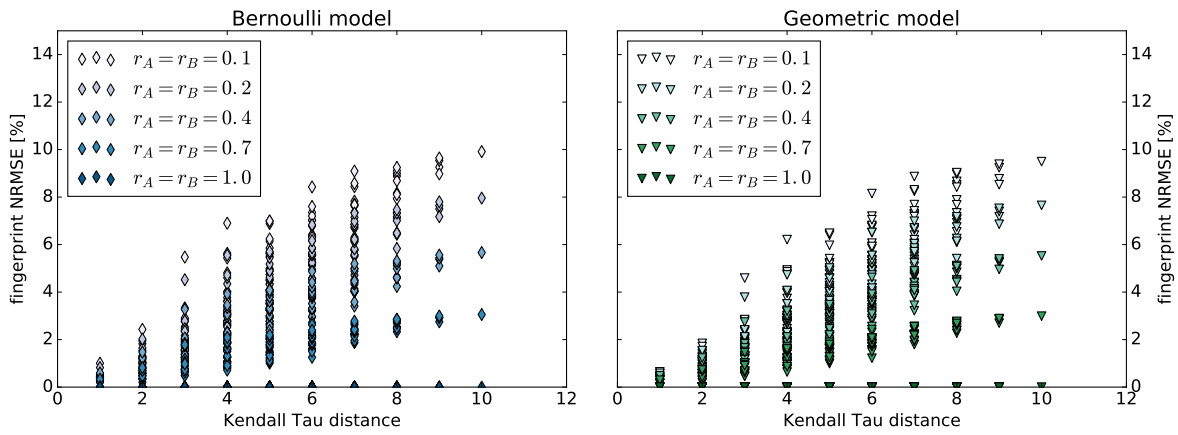


Figure S1. Normalized root mean square errors of the fingerprints for all permutations $\pi(p_A)$ compared to the fingerprint of the original p_A computed with the Bernoulli (left) and Geometric model (right). The Kendall Tau distance is the number of pairwise disagreements between two permutations.

30 step. As previously described by Engler *et al.* [1], the probability of adding i monomers A and j
 31 monomers B to a copolymer chain is given for $a > 0$, $b > 0$, and $1 \leq t \leq T$ as:

$$P(M_{a,b} \rightarrow M_{a+i,b+j}|t) = \binom{i+j}{j} \cdot P_G(i+j) \cdot p_A(t)^i \cdot p_B(t)^j \quad (2)$$

32 We define $f_{i,j}^{a,b}$ as:

$$f_{i,j}^{a,b} = \binom{a+b-i-j}{b-j} \cdot P_G(a+b-i-j) \quad (3)$$

33 Now we apply Eq. 2 and Eq. 3 to find a closed form expression for a fingerprint entry $M_{a,b}$:

$$M_{a,b}(t) = \sum_{i=0}^a \sum_{j=0}^b f_{i,j}^{a,b} \cdot p_A(t)^{a-i} \cdot p_B(t)^{b-j} \cdot M_{i,j}(t-1) \quad (4)$$

34 Now that we are given the equations for computing an entry in the fingerprint at a specific
 35 synthesis step for both models without reactivity parameters, we can show that an inversion of
 36 neighboring values in p_A does not change the resulting fingerprint.

37 **Lemma 1.** Given the Bernoulli model without reactivity parameters and a permutation $\pi(p_A)$ that swaps
 38 $p_A(t)$ with $p_A(t-1)$, then $M_{a,b}(t) = M_{a,b}^\pi(t)$ holds for all $a > 0$, $b > 0$, and $2 \leq t \leq T$.

39 **Proof.** Inserting $M_{a,b}(t-1)$ into the recursive equation 1 yields:

$$\begin{aligned} M_{a,b}(t) = & p_M^2 \cdot p_A(t) \cdot p_A(t-1) \cdot M_{a-2,b}(t-2) \\ & + p_M^2 \cdot p_B(t) \cdot p_B(t-1) \cdot M_{a,b-2}(t-2) \\ & + p_M^2 \cdot p_A(t) \cdot p_B(t-1) \cdot M_{a-1,b-1}(t-2) \\ & + p_M^2 \cdot p_B(t) \cdot p_A(t-1) \cdot M_{a-1,b-1}(t-2) \\ & + p_M \cdot (1-p_M) \cdot p_A(t) \cdot M_{a-1,b}(t-2) \\ & + p_M \cdot (1-p_M) \cdot p_A(t-1) \cdot M_{a-1,b}(t-2) \\ & + p_M \cdot (1-p_M) \cdot p_B(t) \cdot M_{a,b-1}(t-2) \\ & + p_M \cdot (1-p_M) \cdot p_B(t-1) \cdot M_{a,b-1}(t-2) \\ & + (1-p_M)^2 \cdot M_{a,b}(t-2) \end{aligned} \quad (5)$$

40 We replace $p_A(t-1)$ with $\pi(p_A)(t)$, $p_A(t)$ with $\pi(p_A)(t-1)$, $p_B(t-1)$ with $\pi(p_B)(t)$, and $p_B(t)$
41 with $\pi(p_B)(t-1)$:

$$\begin{aligned}
M_{a,b}(t) = & p_M^2 \cdot \pi(p_A)(t) \cdot \pi(p_A)(t-1) \cdot M_{a-2,b}(t-2) \\
& + p_M^2 \cdot \pi(p_B)(t) \cdot \pi(p_B)(t-1) \cdot M_{a,b-2}(t-2) \\
& + p_M^2 \cdot \pi(p_A)(t) \cdot \pi(p_B)(t-1) \cdot M_{a-1,b-1}(t-2) \\
& + p_M^2 \cdot \pi(p_B)(t) \cdot \pi(p_A)(t-1) \cdot M_{a-1,b-1}(t-2) \\
& + p_M \cdot (1-p_M) \cdot \pi(p_A)(t) \cdot M_{a-1,b}(t-2) \\
& + p_M \cdot (1-p_M) \cdot \pi(p_A)(t-1) \cdot M_{a-1,b}(t-2) \\
& + p_M \cdot (1-p_M) \cdot \pi(p_B)(t) \cdot M_{a,b-1}(t-2) \\
& + p_M \cdot (1-p_M) \cdot \pi(p_B)(t-1) \cdot M_{a,b-1}(t-2) \\
& + (1-p_M)^2 \cdot M_{a,b}(t-2)
\end{aligned} \tag{6}$$

42 We simplify the equation to:

$$\begin{aligned}
M_{a,b}(t) = & p_M \cdot \pi(p_A)(t) \cdot M_{a-1,b}(t-1) \\
& + p_M \cdot \pi(p_B)(t) \cdot M_{a,b-1}(t-1) \\
& + (1-p_M) \cdot M_{a,b}(t-1)
\end{aligned} \tag{7}$$

43 Which can be further simplified to:

$$M_{a,b}(t) = M_{a,b}^\pi(t) \tag{8}$$

44 □

45 **Lemma 2.** Given the Geometric model without reactivity parameters and a permutation $\pi(p_A)$ that swaps
46 $p_A(t)$ with $p_A(t-1)$, then $M_{a,b}(t) = M_{a,b}^\pi(t)$ holds for all $a > 0$, $b > 0$, and $2 \leq t \leq T$.

47 **Proof Sketch.** Inserting $M_{i,j}(t-1)$ into the recursive equation 4 yields:

$$\begin{aligned}
M_{a,b}(t) = & \sum_{i=0}^a \sum_{j=0}^b f_{i,j}^{a,b} \cdot p_A(t)^{a-i} \cdot p_B(t)^{b-j} \\
& \cdot \sum_{k=0}^i \sum_{l=0}^j f_{k,l}^{i,j} p_A(t-1)^{i-k} \cdot p_B(t-1)^{j-l} \cdot M_{k,l}(t-2)
\end{aligned} \tag{9}$$

48 Writing the terms of the sums explicitly yields a large equation of the following form:

$$\begin{aligned}
M_{a,b}(t) = & f_{0,0}^{a,b} p_A(t)^a p_B(t)^b \\
& + f_{0,1}^{a,b} p_A(t)^a p_B(t)^{b-1} \left(f_{0,0}^{0,1} M_{0,0}(t-2) + f_{0,1}^{0,1} p_B(t) M_{0,1}(t-2) \right) \\
& + f_{1,0}^{a,b} p_A(t)^{a-1} p_B(t)^b \left(f_{0,0}^{1,0} M_{0,0}(t-2) + f_{1,0}^{1,0} p_A(t) M_{1,0}(t-2) \right) \\
& + f_{1,1}^{a,b} p_A(t)^{a-1} p_B(t)^{b-1} \left(f_{0,0}^{1,1} M_{0,0}(t-2) + f_{1,0}^{1,1} p_A(t) M_{1,0}(t-2) \right. \\
& \quad \left. + f_{0,1}^{1,1} p_B(t) M_{0,1}(t-2) + f_{1,1}^{1,1} p_A(t) p_B(t) M_{1,1}(t-2) \right) \\
& + \dots \\
& + f_{a,b}^{a,b} \left(f_{0,0}^{a,b} M_{0,0}(t-2) + \dots + f_{a,b}^{a,b} p_A(t-1)^a p_B(t-1)^b M_{a,b}(t-2) \right)
\end{aligned} \tag{10}$$

49 If we now expand this equation, we see that for every term of the form $p_A(t)^\alpha p_B(t)^\beta p_A(t-1)^\gamma p_B(t-1)^\delta$
50 there is a corresponding term $p_A(t)^\gamma p_B(t)^\delta p_A(t-1)^\alpha p_B(t)^\beta$ and we change equation 9
51 to:

$$M_{a,b}(t) = \sum_{i=0}^a \sum_{j=0}^b f_{i,j}^{a,b} \cdot p_A(t-1)^{a-i} \cdot p_B(t-1)^{b-j} \cdot \sum_{k=0}^i \sum_{l=0}^j f_{k,l}^{i,j} p_A(t)^{i-k} \cdot p_B(t)^{j-l} \cdot M_{k,l}(t-2) \quad (11)$$

52 We replace $p_A(t-1)$ with $\pi(p_A)(t)$, $p_A(t)$ with $\pi(p_A)(t-1)$, $p_B(t-1)$ with $\pi(p_B)(t)$, and $p_B(t)$
53 with $\pi(p_B)(t-1)$:

$$M_{a,b}(t) = \sum_{i=0}^a \sum_{j=0}^b f_{i,j}^{a,b} \cdot \pi(p_A)(t)^{a-i} \cdot \pi(p_B)(t)^{b-j} \cdot \sum_{k=0}^i \sum_{l=0}^j f_{k,l}^{i,j} \pi(p_A)(t-1)^{i-k} \cdot \pi(p_B)(t-1)^{j-l} \cdot M_{k,l}(t-2) \quad (12)$$

54 We simplify the equation to:

$$M_{a,b}(t) = M_{a,b}^{\pi}(t) \quad (13)$$

55 □

56 For the models without reactivity parameters, we know from Lemma 1 and 2 that no inversion
57 of neighboring values in p_A changes the resulting fingerprint. Any permutation of a vector can be
58 constructed by a sequence of inversions of neighboring elements. Therefore, for the Bernoulli and
59 Geometric model without reactivity parameters, all permutations of a probability vector p_A have the
60 same resulting fingerprint.

61 3. Parameter optimization

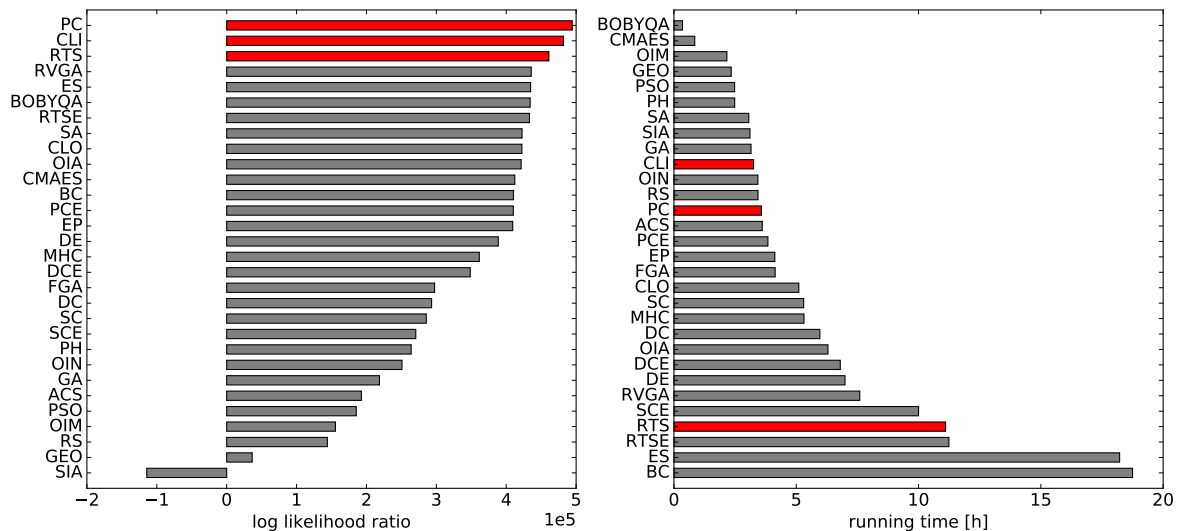


Figure S2. Left: Log likelihood ratio of all optimization algorithms using the direct method on the $DP_n = 3, r_A = 2.0$ instance without noise. The top three algorithms are marked in red. Right: Running times of the algorithms.

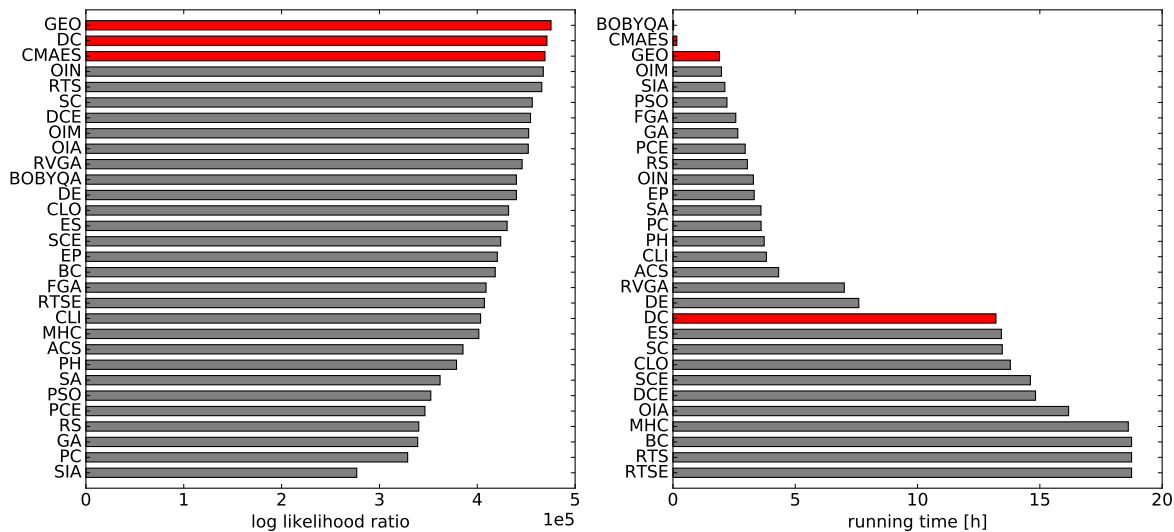


Figure S3. Left: Log likelihood ratio of all optimization algorithms using the spline method on the $DP_n = 3, r_A = 2.0$ instance without noise. The top three algorithms are marked in red. Right: Running times of the algorithms.

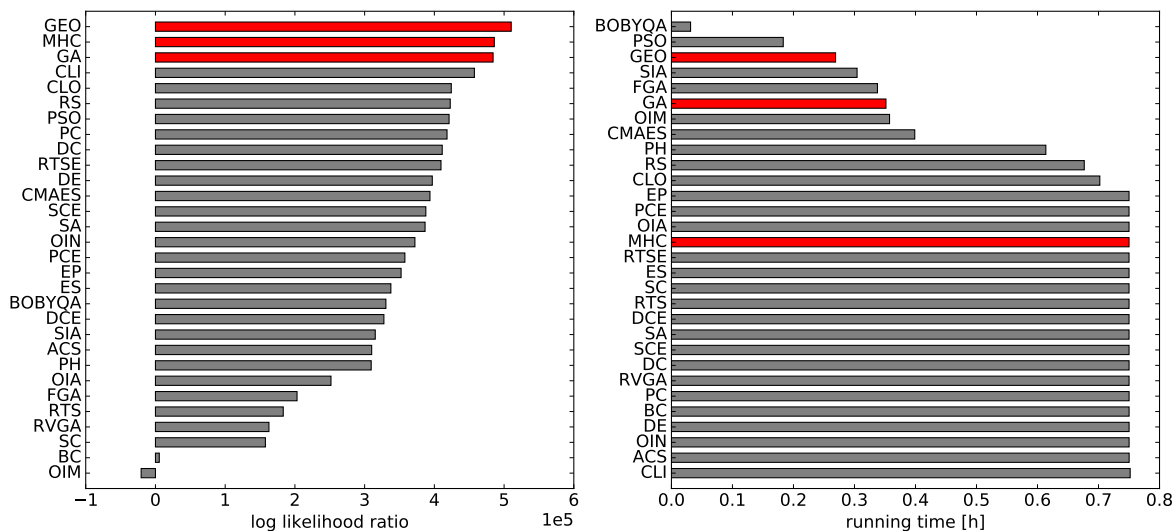


Figure S4. Left: Log likelihood ratio of all optimization algorithms using the ODE method on the $DP_n = 3, r_A = 2.0$ instance without noise. The top three algorithms are marked in red. Right: Running times of the algorithms.

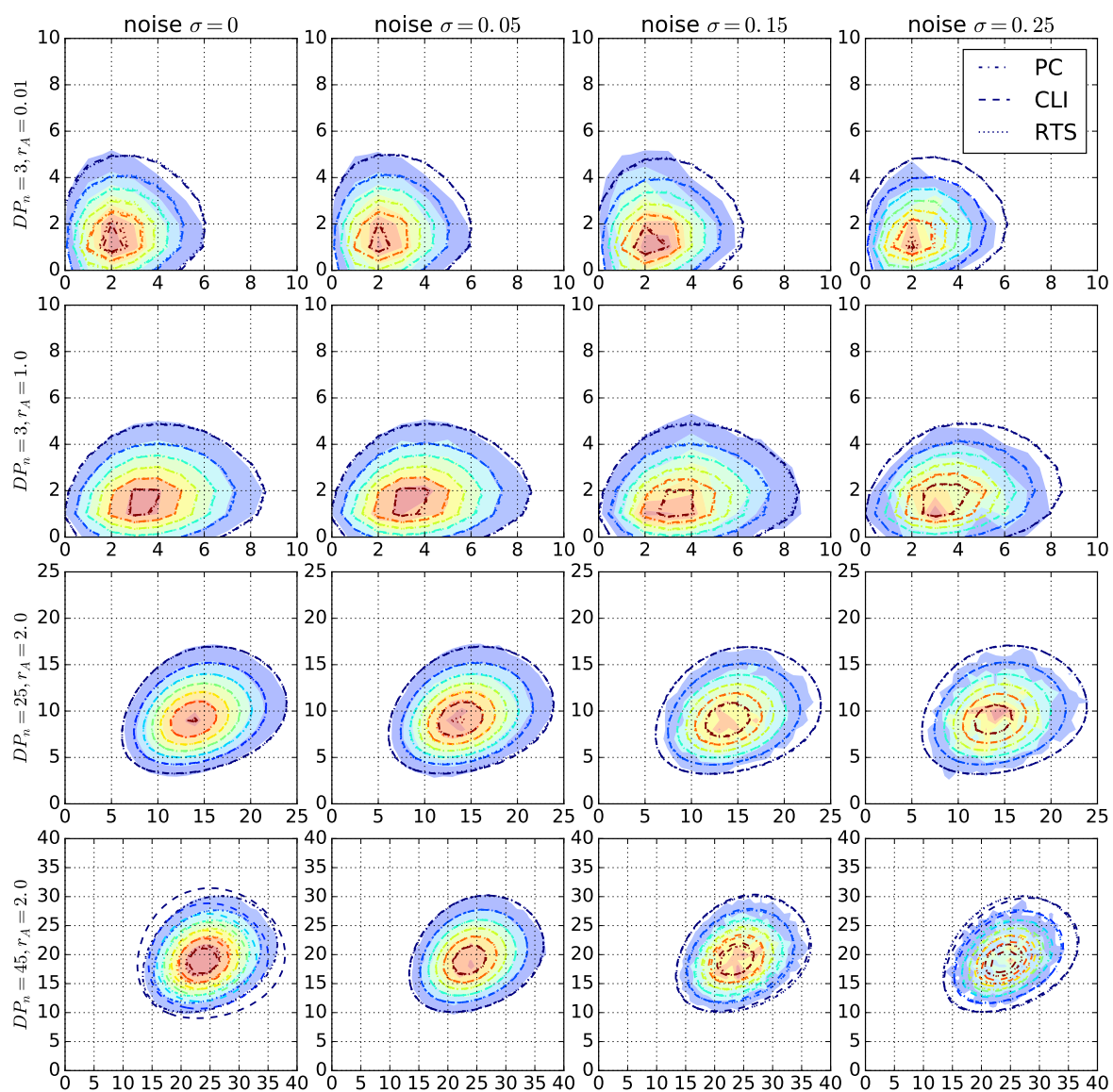


Figure S5. Filled contours: Fingerprints of the datasets $DP_n = 3, r_A = 0.01$, $DP_n = 3, r_A = 1.0$, $DP_n = 25, r_A = 2.0$, and $DP_n = 45, r_A = 2.0$, (top to bottom) with increasing noise (left to right). Contours: Fingerprints computed by the model using the direct method.

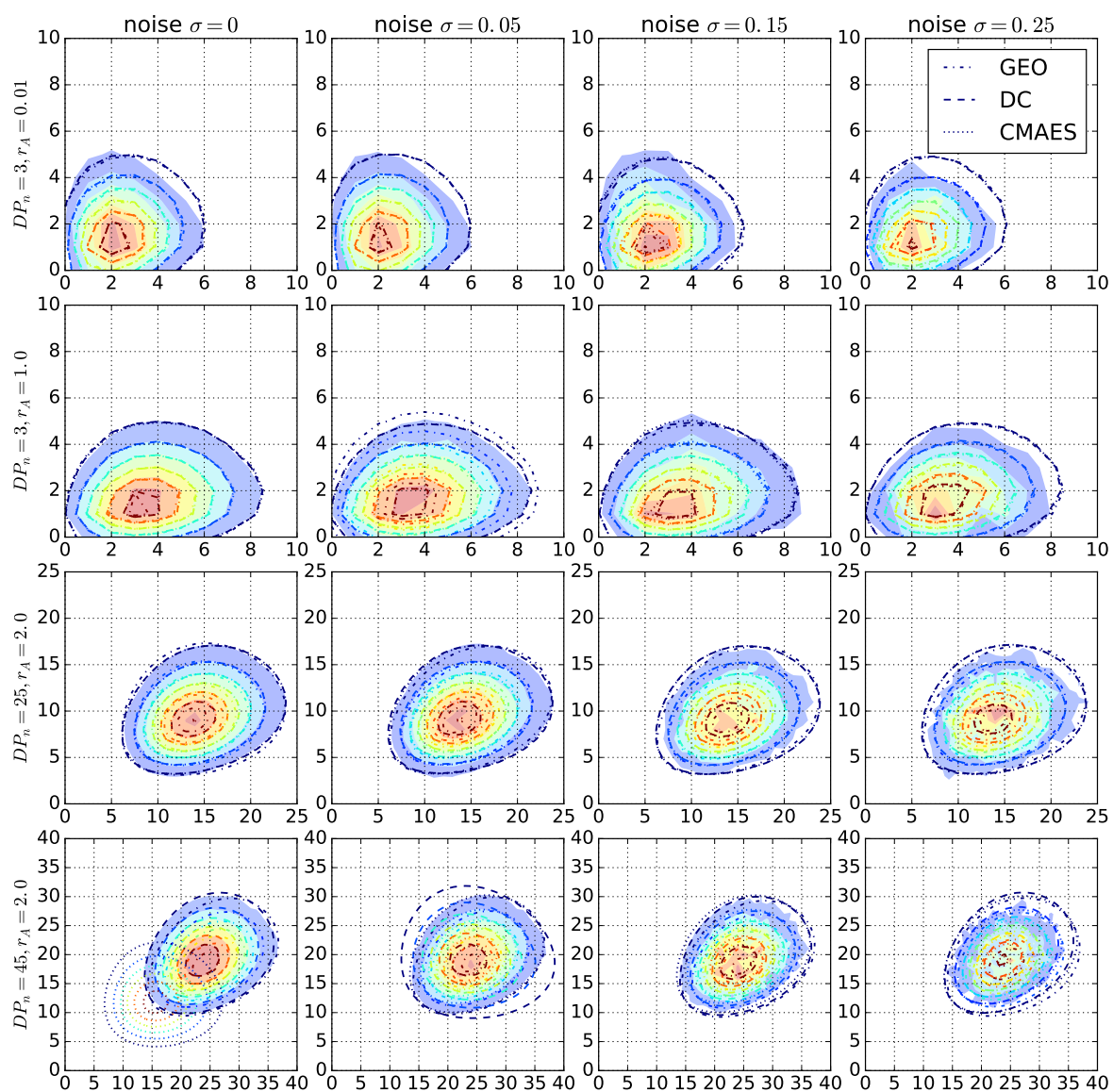


Figure S6. Filled contours: Fingerprints of the datasets $DP_n = 3, r_A = 0.01$, $DP_n = 3, r_A = 1.0$, $DP_n = 25, r_A = 2.0$, and $DP_n = 45, r_A = 2.0$ (top to bottom) with increasing noise (left to right). Contours: Fingerprints computed by the model using the spline method.

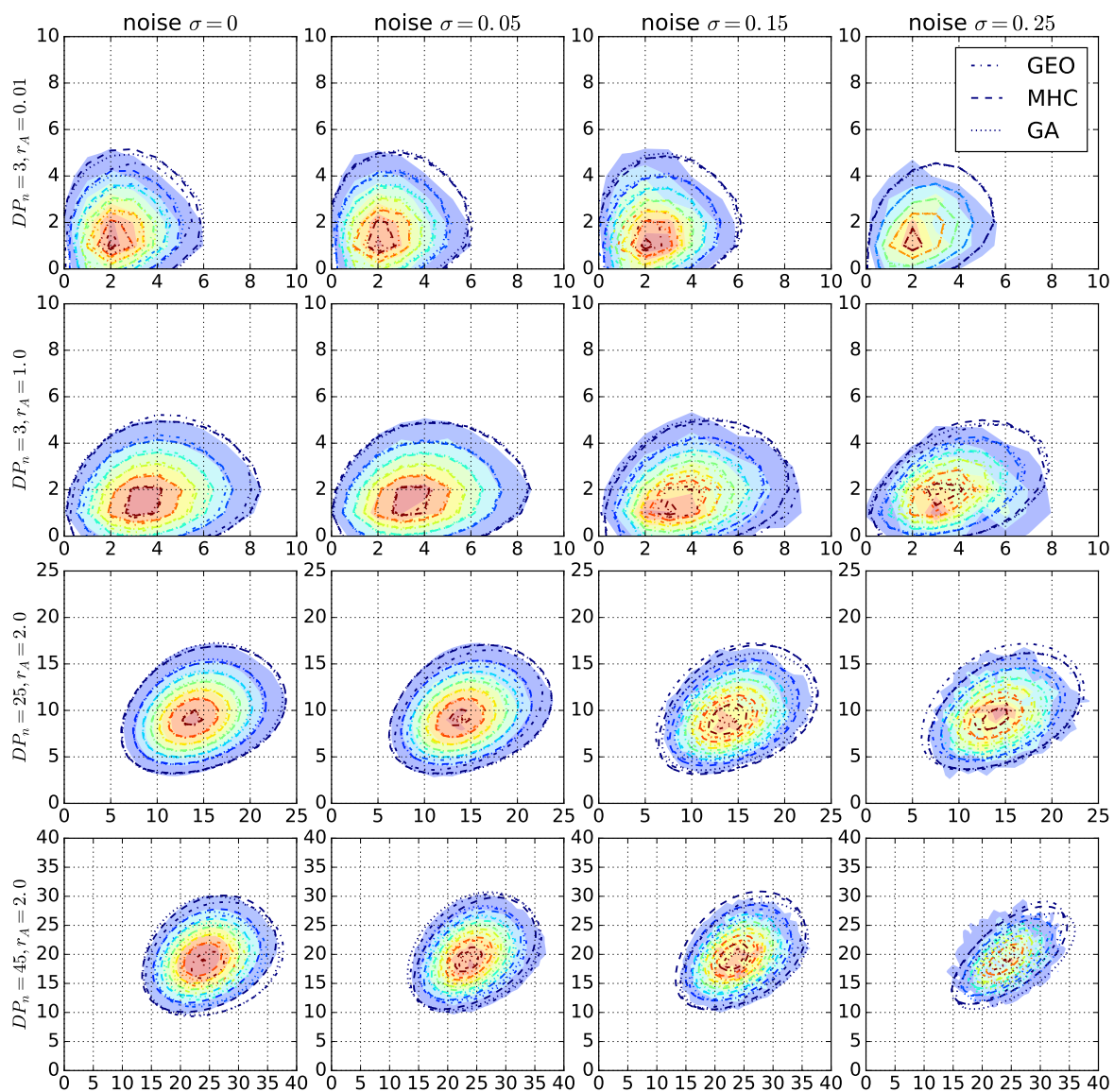


Figure S7. Filled contours: Fingerprints of the datasets $DP_n = 3, r_A = 0.01$, $DP_n = 3, r_A = 1.0$, $DP_n = 25, r_A = 2.0$, and $DP_n = 45, r_A = 2.0$, (top to bottom) with increasing noise (left to right). Contours: Fingerprints computed by the model using the ODE method.

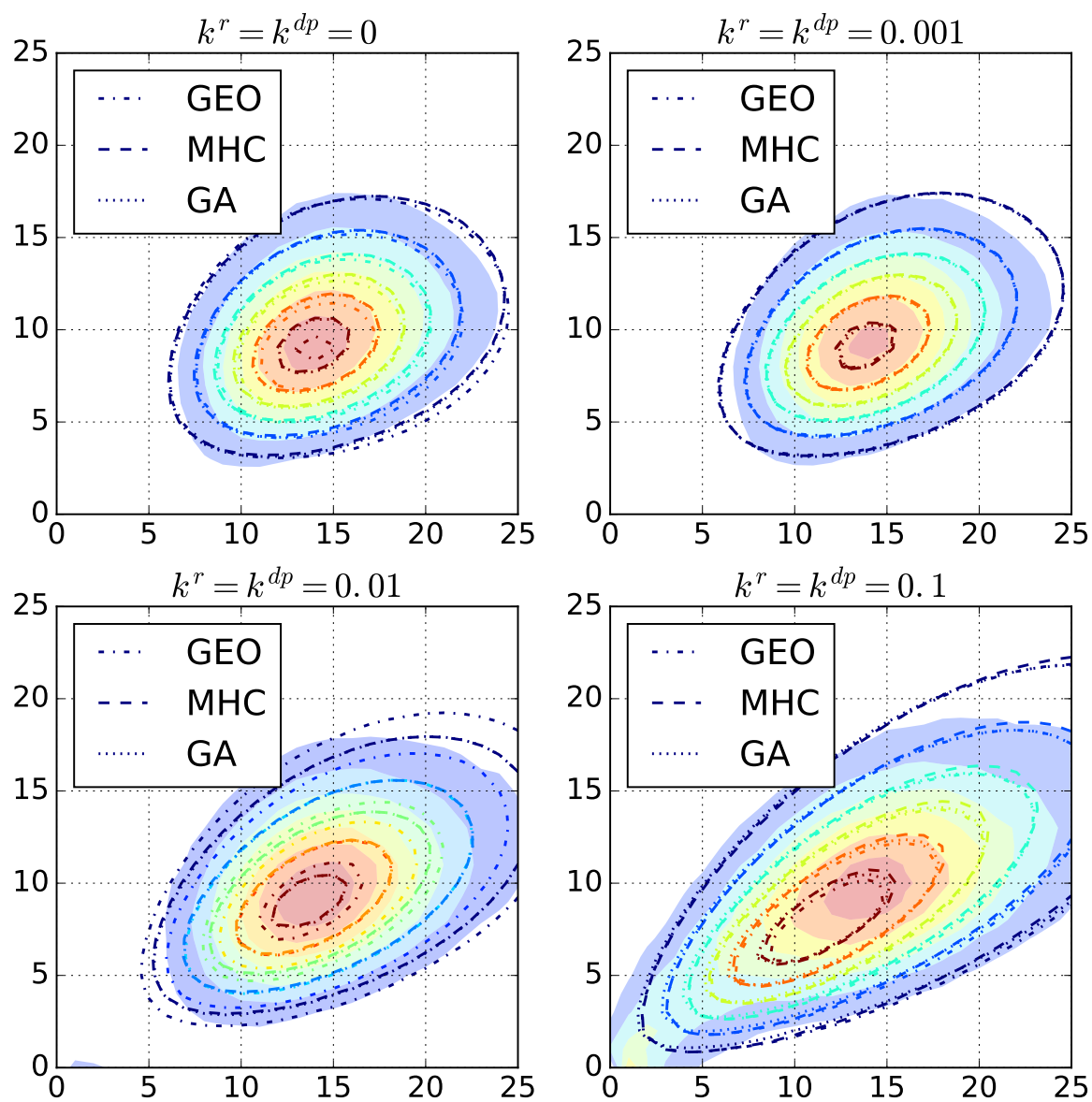


Figure S8. Filled contours: Fingerprints of the controlled radical copolymerizations with increasing recombination k^r and disproportionation rates k^{dp} . Contours: Fingerprints computed by the model using the ODE method.

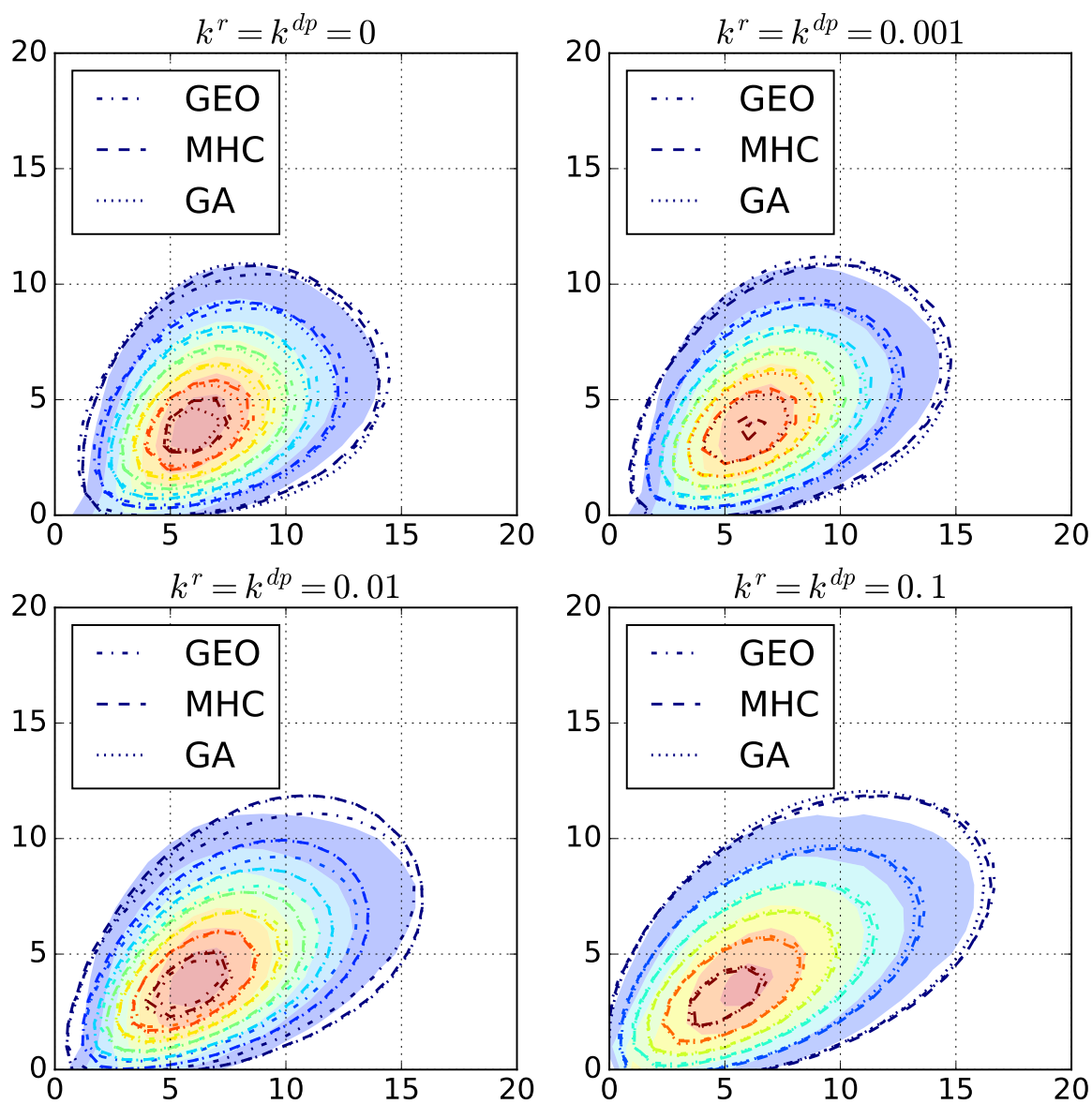


Figure S9. Filled contours: Fingerprints of the free radical copolymerizations with increasing recombination k^r and disproportionation rates k^{dp} . Contours: Fingerprints computed by the model using the ODE method.

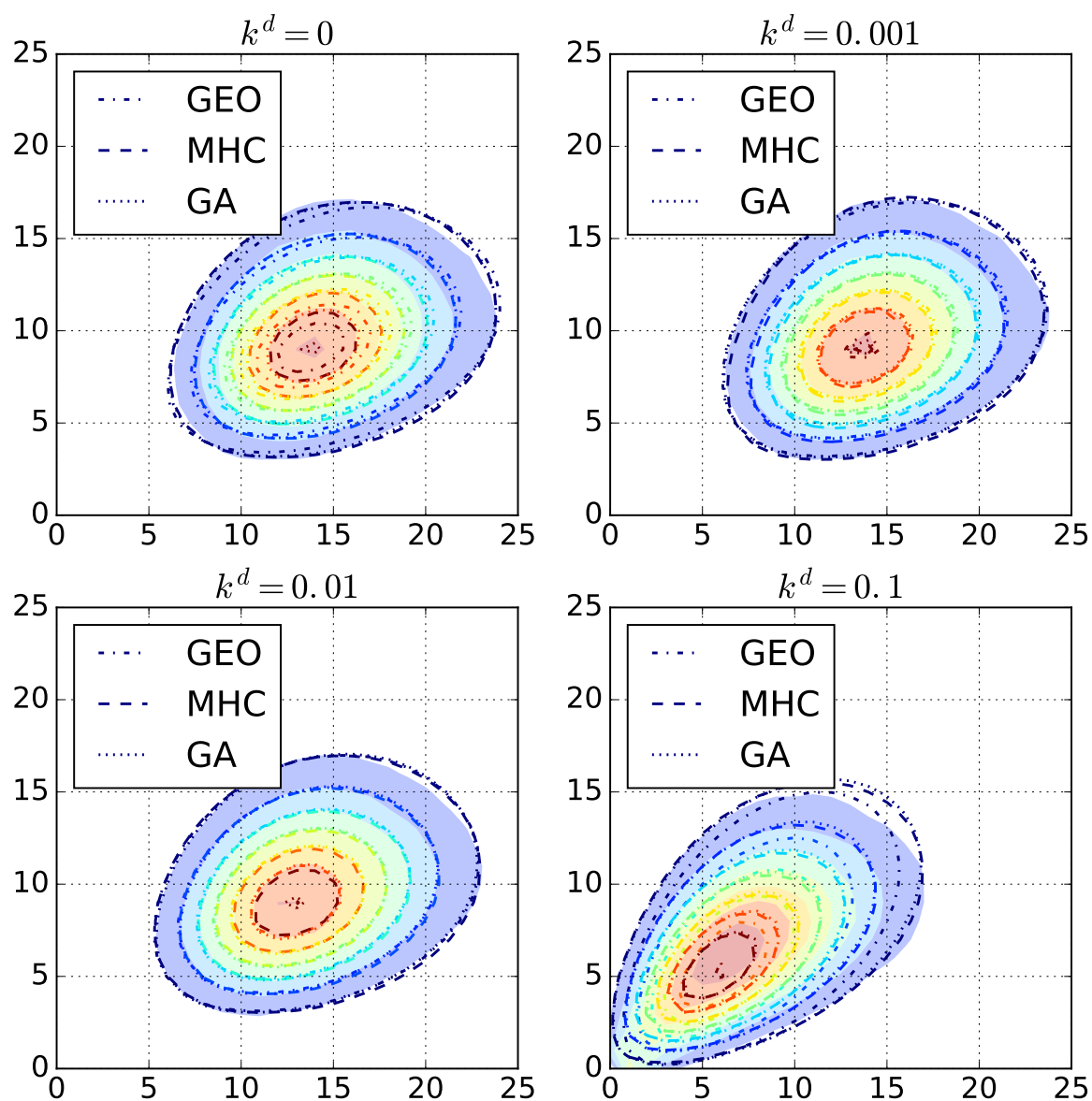


Figure S10. Filled contours: Fingerprints of the reversible living copolymerizations with increasing depropagation rates k^d . Contours: Fingerprints computed by the model using the ODE method.

62 Bibliography

- 63** 1. Engler, M.S.; Scheubert, K.; Schubert, U.S.; Böcker, S. New Statistical Models for Copolymerization.
64 *Polymers* **2016**, *8*, 240.